

# Colored noise, folding rates and departure from Kramers' behavior

Bidhan Chandra Bag,<sup>a</sup> Chin-Kun Hu<sup>bc</sup> and Mai Suan Li<sup>\*d</sup>

Received 10th March 2010, Accepted 29th June 2010

DOI: 10.1039/c004113k

Recent experiments have shown that, for several proteins, the dependence of folding and unfolding rates on solvent viscosity does not obey Kramers' theory. Such a departure from standard Kramers' behavior is often attributed to the existence of internal friction, related to the structure of a polypeptide chain. In this paper, we propose an entirely different mechanism leading to violation of Kramers' theory. Using the generalized Langevin equation with time-dependent friction and a  $C_\alpha$ -Go model, we demonstrate that this effect *may be* caused by the colored Gaussian noise which is characterized by correlation time  $\tau$ . Surprisingly, the dependence of folding time  $t_f$  on  $\tau$  is non-trivial: the plot  $t_f$  vs  $\tau$  exhibits two minima at low and intermediate values of  $\tau$ . The appearance of one more additional minimum is in sharp contrast to one dimensional barrier crossing dynamics. We argue that it is a generic signature of entropy of activation in a multidimensional problem.

## 1. Introduction

Despite numerous advances in recent years,<sup>1,2</sup> the protein folding problem remains one of the biggest challenges in molecular biology. It is well known that in addition to the intrinsic sequence properties, the external conditions like temperature, pH, salt concentration, confinement, viscosity of the medium, *etc.* have a profound effect on protein folding rates.<sup>3,4</sup> For example, from computational studies it follows that the dependence of the folding time,  $t_f$ , on temperature,<sup>5-7</sup> viscosity<sup>8-10</sup> and size of confinement<sup>11</sup> has a U-shape. In the temperature dependence case, at low temperatures (energy-driven regime),  $t_f$  is large due to energetic traps and it becomes smaller as  $T$  is increased. However, at sufficiently high  $T$  (entropy-driven regime),  $t_f$  grows again as the entropy factor dominates over the energetic one. The effect of environment crowding,<sup>12</sup> viscosity,<sup>13-17</sup> and temperature<sup>18</sup> on the folding kinetics was studied experimentally. However, the U-shape behavior has not been observed by experiments because they were performed for restrict intervals of parameters.

Protein folding kinetics is an example of thermally activated barrier crossing dynamics in a multidimensional system. Experimental studies in eighties<sup>19,20</sup> imply that Markovian dynamics can not accurately account for the effect of viscosity on the barrier crossing phenomenon in the solution phase. However, the theory developed focusing on non-Markovian dynamics (NMD)<sup>20-23</sup> shows a fair agreement between theoretical and experimental results. It is particularly relevant when the motion near the top of the barrier takes place on a picosecond or subpicosecond time scale, the solvent forces at

two different times can become correlated; *i.e.*, memory effects become important and Kramers' theory can break down (experimental work has given evidence for such failure<sup>24-26</sup>). The contribution from the NMD may be meaningful if the barrier crossing time is of the order of solvent relaxation time (picosecond). In other words, for large barrier crossing time compared to picosecond order this contribution may be negligible and then Kramers' approximation should be good. Thus for the folding kinetics of a large protein molecule (whose free energy barrier is high) at high viscosity Kramers' approximation may be very accurate. For small protein molecule and low viscosity there may be deviation from it. However, another more likely reason for the breakdown of one dimensional Kramers' theory for the multi dimensional barrier crossing problem is the non-Markovian configurational diffusion.<sup>31</sup> The NMD of protein chains may have an important role in the folding kinetics of the native state and lead to deviations in the barrier crossing rate from Kramers' theory. We will discuss it in more detail during the explanation of our results. Since protein folding time depends on the viscosity,<sup>8-10</sup> studying the effect of NMD on protein folding kinetics in the condensed phase should be a worthy issue.

Much of the investigation of the role of friction on protein folding and unfolding has been based on examining the effect of solvent viscosity on rates of structural transitions using Kramers' theory.<sup>27</sup> Assuming that barrier crossing occurs through Brownian motion of a polypeptide chain, this theory predicts that, in the high friction regime, the folding rate,  $k_f$ , is inversely proportional to the solvent friction,  $\gamma_0$ , *i.e.*,  $k_f = \frac{C}{\gamma_0}$ , where  $C$  is a constant. This prediction has been confirmed by simulations<sup>8</sup> using Markovian dynamics for model proteins as well as by experiments for some proteins.<sup>28,29</sup> However, for other proteins,<sup>13,14</sup> a modification of Kramers' theory is required to describe the dependence of folding rates on the friction. Namely, in order to get good fitting to experimental data, one uses the following formula:<sup>13-17</sup>

$$k_f = \frac{C}{\gamma_0 + \xi} \quad (1)$$

<sup>a</sup> Department of Chemistry, Visva-Bharati, Santiniketan, India. E-mail: bidhanchandra.bag@visva-bharati.ac.in

<sup>b</sup> Institute of Physics, Academia Sinica, Nankang, Taipei 11529, Taiwan

<sup>c</sup> Center for Nonlinear and Complex Systems and Department of Physics, Chung-Yuan Christian University, Chungli 32023, Taiwan

<sup>d</sup> Institute of Physics, Polish Academy of Sciences, Aleja Lotnikow 32/46, 02-668 Warsaw, Poland. E-mail: masli@ifpan.edu.pl; Fax: +48 22 8475223; Tel: +48 22 8436601

The nature of the adjustable parameter  $\zeta$  remains controversial. From unfolding rates obtained for the protein barstar,<sup>14</sup> it follows that  $\zeta < 0$ . However, the folding experiments on the 36-residue villin headpiece subdomain,<sup>15</sup> the tryptophane cage,<sup>16</sup> and myoglobin<sup>17</sup> suggest that  $\zeta > 0$ . One of possible reasons for reduction of viscosity, described by negative values of  $\zeta$ , is that the local viscosity at the protein–solvent interface is lower than the bulk solvent viscosity.<sup>30</sup> In the experiments of Pradeep *et al.*<sup>14</sup> the change in the folding barrier by viscogen is compensated by addition of denaturant, the variation of folding rates is, therefore, solely defined by the viscosity. Based on this, it was also assumed that the violation of Kramers' theory with  $\zeta > 0$  is due to internal friction.<sup>13,14</sup> The nature of this friction is presumably related to the fact that only small parts of a polypeptide chain are involved in the rate-limiting step of folding.

In the experiments by Cellmer *et al.*,<sup>15</sup> chemical denaturants were not used, but the folding and unfolding barriers of the ultra-fast folding villin headpiece subdomain are not affected by viscogen remaining constant within experimental error. In this very special case, the negative value of  $\zeta$  is attributed to the increase of the effective viscosity, which is probably associated with a shift of the transition state along the reaction coordinate toward the native state.<sup>15</sup> In other words, the reduction of the diffusion coefficient is due to increased free energy landscape roughness.

To our best knowledge, at a quantitative level, no theoretical attempts has been undertaken to understand the nature of parameter  $\zeta$  thus far. This is probably because the calculation of viscosity experienced by a protein during folding process from first principles is not an easy task. Therefore, the question we ask is whether the departure from Kramers' behavior (eqn (1)) observed in folding/unfolding experiments is caused by a noise memory effect. This is a main motivation for studying the protein folding in the presence of colored noise. It should be noted that the influence of noise correlation on folding kinetics was studied before,<sup>31</sup> but this important question was not addressed.

Using the  $C_\alpha$ -Go model<sup>32</sup> and the generalized Langevin equation with colored noise,<sup>20</sup> we have shown that the deviation from Kramers' behavior (eqn (1)) is due to NMD. This key result of our work is very important as we are the first to point out that the noise correlation is responsible for non-Kramers unfolding kinetics observed in experiments with  $\zeta < 0$ .<sup>13,14</sup>

Our second interesting result is that the dependence of folding time  $t_f$  on the memory time  $\tau$  displays the double U-shape (two minima), opposed to the standard single U-shape mentioned above. Employing several model systems, we have demonstrated that one of these minima occurs due to the interplay of the frequency corresponding to the curvature of the potential well, damping and the noise correlation time, while the other one is due to the interplay of damping, color noise and entropy of activation. Moreover, at optimal values of  $\tau$ , the folding speeds up by nearly a factor of two.

## 2. Models and methods

### Coarse-grained model for proteins

The conformation of a polypeptide chain in a coarse-grained representation is specified by a set of coordinates

$\vec{r}_i (i = 1, \dots, N)$  of the  $C_\alpha$ -carbon atoms where  $N$  is a number of amino acids. The energy of a conformation for the  $C_\alpha$ -Go model is<sup>32</sup>

$$E = \sum_{\text{bonds}} \frac{K_r}{2} (r_i - r_{0i})^2 + \sum_{\text{angles}} \frac{K_\theta}{2} (\theta_i - \theta_{0i})^2 + \sum_{\text{dihedral}} \{K_\phi^{(1)} [1 - \cos(\phi_i - \phi_{0i})] + K_\phi^{(3)} [1 - \cos 3(\phi_i - \phi_{0i})]\} + \sum_{i>j+3}^{NC} \varepsilon_H \left[ 5 \left( \frac{r_{0ij}}{r_{ij}} \right)^{12} - 6 \left( \frac{r_{0ij}}{r_{ij}} \right)^{10} \right] + \sum_{i>j+3}^{NNC} \varepsilon_H \left( \frac{C}{r_{ij}} \right)^{12}, \quad (2)$$

where  $r_i$ ,  $\theta_i$ , and  $\phi_i$  are the bond length between  $i$  and  $i - 1$  residues, the bond angle between  $(i - 1, i)$  and  $(i, i + 1)$  bonds and the dihedral angle around the  $i$ th bond, respectively. Subscript 0 and superscripts NC and NNC refer to native conformation, native contacts and non-native contacts, respectively. Beads  $i$  and  $j$  are in native contact, if they are within a cut-off distance  $d_c = 6.5 \text{ \AA}$ . During simulation a contact between residues  $i$  and  $j$  is formed when  $r_{ij}$  is less than  $1.2 d_c$ . We used the same set of parameters as for Go modeling of ubiquitin,<sup>33</sup>  $K_r = 100\varepsilon_H/a^2$ ,  $K_\theta = 20\varepsilon_H/\text{rad}^2$ ,  $K_\phi^{(1)} = \varepsilon_H$ ,  $K_\phi^{(3)} = 0.5\varepsilon_H$ ,  $\varepsilon_1 = \varepsilon_2 = \varepsilon_H$  and  $C = 4 \text{ \AA}$ , where the hydrogen bond energy  $\varepsilon_H = 0.98 \text{ kcal mol}^{-1}$ .

For illustration we will show the results obtained for the 16-residue peptide  $\beta$ -hairpin (C-terminal from protein G, PDB ID: 2gb1), 36-residue villin (PDB ID: 1vii), 76-residue protein ubiquitin (PDB ID: 1ubq) and protein barstar (PDB ID: 1brs). The PDB structures of these proteins are shown in Fig. 1. The main computations were carried out at  $T = 0.53\varepsilon_H/k_B = 285 \text{ K}$ , which is equal  $\approx 0.86T_F$ , where  $T_F = 332.5 \text{ K}$  is the melting temperature of ubiquitin.<sup>34</sup> At this temperature the folding of ubiquitin follows a two-state scenario.<sup>33</sup> The same also holds for the  $\beta$ -hairpin, villin and barstar (data not shown).

### Langevin dynamics with colored noise

The dynamics of a polypeptide chain in presence of a thermal bath can be described by the following generalized Langevin equation of motion,<sup>20</sup>

$$m\ddot{\vec{r}} = \vec{F}_c - \int_0^t \gamma(t-t')\dot{\vec{r}}(t')dt' + \zeta(t). \quad (3)$$

Here  $m$  is the mass of a bead and  $\vec{F}_c = -\nabla E$ , the energy of the system  $E$  is given by eqn (2). The frictional kernel  $\gamma(t)$  is connected to internal Gaussian noise  $\zeta(t)$  by the well-known fluctuation-dissipation relationship (FDR)

$$\langle \zeta(t)\zeta(t') \rangle = mk_B T \gamma(t-t'). \quad (4)$$

$k_B$  and  $T$  are Boltzmann's constant and the temperature of the system respectively. To capture essential features of the non-Markovian dynamics, we consider an exponentially

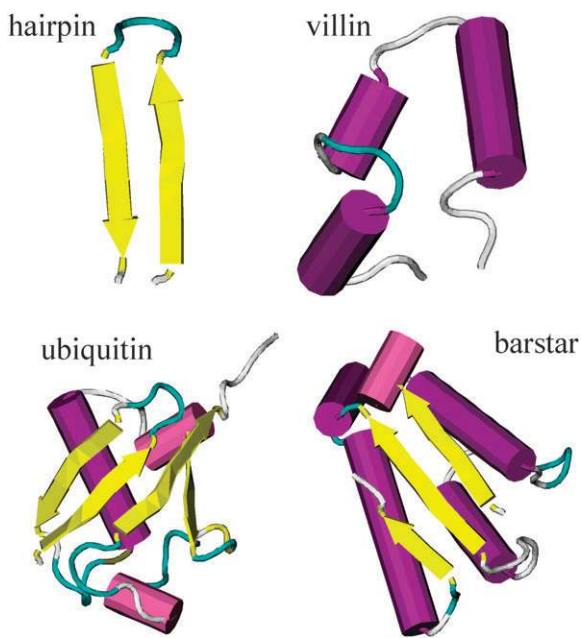


**Fig. 1** The PDB structures of three proteins studied in this work. For the cutoff distance  $d_c = 6.5 \text{ \AA}$ , the total number of native contacts is equal  $Q_{\max} = 13, 26, 99,$  and  $104$  for hairpin, villin, ubiquitin and barstar, respectively.

decaying frictional memory kernel.<sup>23,35,36</sup> Therefore,  $\gamma(t - t')$  in the present model can be represented as,

$$\gamma(t - t') = \frac{\gamma_0}{\tau} e^{-\frac{|t-t'|}{\tau}}, \quad (5)$$

where  $\tau$  is the memory time of the NMD and  $\gamma_0$  is the frictional coefficient in the Markovian limit  $\tau = 0$ . For the frictional memory kernel (4) the integro-differential (3) can read as

$$m\ddot{\vec{r}} = -\vec{F}_c + \zeta(t) \quad (6a)$$

$$\dot{\zeta} = -\zeta/\tau - \gamma_0 \dot{\vec{r}}/\tau + \frac{\sqrt{\gamma_0 k_B T}}{\tau} \xi(t). \quad (6b)$$

Here  $\xi(t)$  is a Gaussian white noise term. The second-order differential eqn (6a) is similar to the standard Langevin equation with white noise, except that  $\zeta(t)$  obeys eqn (6b). To solve eqn (6a), we have tried the second-order velocity Verlet<sup>37</sup> as well as corrector-predictor algorithms.<sup>38</sup> Since both of them give the same results, we chose the first one because of its higher efficiency. Using the Euler method and eqn (6b),  $\zeta(t)$  is updated as follows

$$\zeta(t + \Delta t) = \zeta(t) - \left[ \zeta(t)/\tau + \gamma_0 \dot{\vec{r}}(t)/\tau - \frac{\sqrt{\gamma_0 k_B T}}{\tau} \xi(t) \right] \Delta t. \quad (7)$$

The friction  $\gamma_0$  is measured in the unit of  $\frac{m_a}{\tau_L}$ .<sup>37</sup> Here  $\tau_L = (m_a a^2 / \epsilon_H)^{1/2} \approx 3 \text{ ps}$ , where the characteristic bond length between successive beads  $a \approx 4 \text{ \AA}$  and the typical mass of amino acid residues  $m_a \approx 3 \times 10^{-22} \text{ g}$ .<sup>37</sup> As in previous works,<sup>33,37,39-44</sup> we have chosen the time step  $\Delta t = 0.005\tau_L = 15 \text{ fs}$ . The same folding times were obtained with a shorter time step (5 fs) (data not shown). In order to prepare initial

conformations for the folding simulations, we heated a system up to  $T = 450 \text{ K}$  and performed unfolding simulations at this temperature, starting from the native state, until one obtains unfolded conformations with no native contacts. The folding simulation is initiated from these unfolded conformations and it is terminated when all of the native contacts are formed. The folding time is defined as the averaged value of first passage times which are needed to reach the native state starting from random conformations.

We define the unfolding time,  $t_{uf}$ , as the average of first passage times to reach an extended conformation with no native contacts. Different trajectories start from the same native conformation but with different random number seeds. To obtain good statistics, we have generated 50–1000 independent trajectories for each set of parameters.

### Typical values of noise correlation time

Since the correlated noise is related to the vibrational dynamics of water and proteins, typical values of  $\tau$  at which the NMD becomes relevant should be of the same order of magnitude as characteristic time scales of these processes. The characteristic time scale for the protein vibration  $\tau_v^p \approx 2\pi\sqrt{m_a/K_r^p}$ , where the spring constant  $K_r^p$  is defined by the covalent bond energy. Using a typical value  $K_r^p \approx 100\epsilon_H/a^2$  we obtain  $\tau_v^p \approx 2 \text{ ps}$ . Assuming water is a system of beads connected by hydrogen bonds with the spring constant  $K_r^w = \epsilon_H/\text{\AA}^2$ , we obtain the vibrational time scale for water,  $\tau_v^w \approx 2\pi\sqrt{m_w/K_r^w} \approx 1.2 \text{ ps}$ , where the mass of the water molecule  $m_w \approx 18 \text{ g mol}^{-1} \approx 3 \times 10^{-23} \text{ g}$ . Our rough estimates are consistent with protein<sup>45</sup> and water<sup>46</sup> dynamics experiments which showed that  $\tau_v^p$  and  $\tau_v^w$  are of order of picoseconds. Therefore, the NMD is relevant if  $\tau \sim (\tau_v^p, \tau_v^w)$ , or  $\tau$  should be of a few picoseconds. These typical values of  $\tau$  are used in our simulations. To make it physically more clear we note that in the Brownian motion the tagged particle is coupled to the bath modes of vibration and their collective effect on the particle is the Langevin equation of motion. The Fourier transform of the two time correlation functions of the random force depends upon the frequency distribution of the bath modes.<sup>20</sup> It is obvious if the medium is incompressible, like water, then the frequency distribution must have a cut-off; the noise process is then called colored noise and dissipation in the Langevin equation should be present as a memory kernel (eqn (3)). It is also then obvious that the memory time depends on the collective dynamics of the constituents of the medium. Therefore, for water as a thermal bath the memory time should be of same order of magnitude as that of  $\tau_v^w$ .

### Grote–Hynes theory

Extending Kramers' approach to the time-dependent friction case, Grote and Hynes<sup>21</sup> developed the rate theory for non-Kramers dynamics. They obtained the following approximate expression for the barrier crossing rate

$$k = \frac{\omega_1 \omega_2}{2\pi \left( \lambda_r + \frac{f(\lambda_r)}{m} \right)} \exp\left(-\frac{E_a}{RT}\right), \quad (8)$$

where

$$f(\lambda_r) = \frac{1}{k_B T} \int_0^\infty \langle \zeta(t)\zeta(0) \rangle \exp(-\lambda_r t) dt. \quad (9)$$

Parameter  $\lambda_r$  reflects the unstable reactive motion in the barrier region.<sup>21</sup>  $E_a$  is the energy barrier,  $\omega_1$  and  $\omega_2$  the curvatures at the reactant bottom and at the barrier top,<sup>27</sup> respectively. Using eqn (4) and (5) in the above equation we have

$$f(\lambda_r) = m \frac{\gamma_0}{1 + \lambda_r \tau} \quad (10)$$

Substituting this equation into eqn (8), we obtain

$$k = \frac{\omega_1 \omega_2}{2\pi \left( \lambda_r + \frac{\gamma_0}{1 + \lambda_r \tau} \right)} \exp\left(-\frac{E_a}{RT}\right). \quad (11)$$

This formula will be used to understand the experimental and simulation results on the qualitative level.

In fitting simulation data, obtained at a given value of  $T$ , we use the following form of the formula (11):

$$k = \frac{\tilde{k}_0}{\lambda_r + \frac{\gamma_0}{1 + \lambda_r \tau}}, \quad (12)$$

$$\tilde{k}_0 = \frac{\omega_1 \omega_2 \exp\left(-\frac{E_a}{RT}\right)}{2\pi},$$

where  $\lambda_r$  and  $\tilde{k}_0$  are treated as two free parameters.

### 3. Results and discussions

#### Dependence of folding times on noise correlation time displays two minima

The dependence of  $t_f$  on  $\tau$  is shown for the  $\beta$ -hairpin (Fig. 2) and ubiquitin (Fig. 3) for friction  $\gamma_0 = 0.1, 2$  and  $5 \text{ ps}^{-1}$ . For large damping ( $\gamma_0 = 50 \text{ ps}^{-1}$ ), the result is demonstrated in Fig. 4. For  $\gamma_0 = 0.1 \text{ ps}^{-1}$ , at the first minimum the folding of ubiquitin speeds up about two-fold compared to Markovian dynamics ( $\tau = 0$ ). The maximum enhancement of folding rates of the hairpin is smaller than that of ubiquitin (results not shown). The effect is expected to become more pronounced as the size of proteins increases, because it would lead to an increase in folding times.<sup>41,47</sup> Thus, for all values of  $\gamma_0$ , we have observed the surprising result that there exist two minima. This result also holds for the 89-residue titin domain I27 (results not shown). In the next section, we will show that the result is robust for all the proteins.

#### Nature of two minima

Since the double U-shape of dependence of  $t_f$  on external parameters was not reported in any previous studies, it is vital to understand the origin of two minima in Fig. 2 and 3. For this we invoke the barrier crossing problem in a one-degree-of-freedom (ODF) system using the same non-Markovian thermal bath. Here, we consider a single particle moving in a two dimensional phase space with the FDR kept constant. This system will be referred to as model A. The folding time, defined as a mean first barrier crossing time, was obtained by solving the Langevin equation of motion,

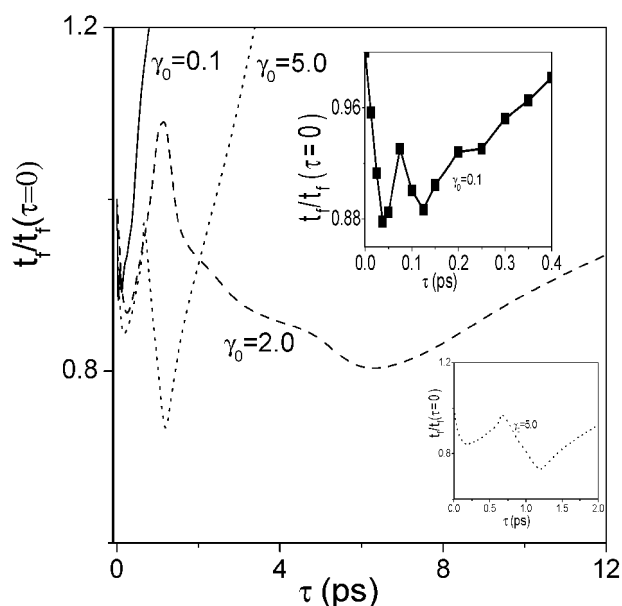


**Fig. 2** Plot of the renormalized folding time  $t_f/t_f(0)$  vs. the noise correlation times for hairpin, where  $t_f(0)$  is the folding time in the Markovian limit,  $\tau = 0$ . We choose  $\gamma_0 = 0.1$  (solid curve), 2 (dashed curve) and 5 (dotted curve) and  $T = 285 \text{ K}$ .  $t_f(0)$  for  $\gamma = 0.1, 2$  and 5 are 0.23 ns, 1.6 ns and 4.1 ns respectively. The upper inset shows the results for  $\gamma_0 = 0.1$  at small values of  $\tau$ . The results are averaged over 500 trajectories, and the error bars are smaller than the data symbols. The lower inset is the same as in the upper inset, but for  $\gamma_0 = 5$ .

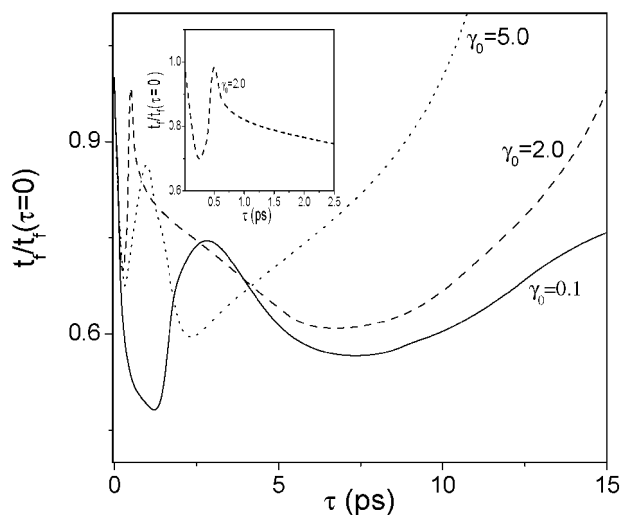


**Fig. 3** Plot of the renormalized folding time  $t_f/t_f(0)$  vs. the noise correlation times for ubiquitin, where  $t_f(0)$  is the folding time in the Markovian limit,  $\tau = 0$ . We choose  $\gamma_0 = 0.1$  (solid curve), 2 (dashed curve) and 5 (dotted curve) and  $T = 285 \text{ K}$ .  $t_f(0)$  for  $\gamma_0 = 0.1, 2$  and 5 are 20.01 ns, 110.1 ns, and 261.085 ns respectively. The inset shows the low  $\tau$  results for  $\gamma_0 = 2$ .

$m\dot{v} = q - q^3 - \int_0^t \gamma(t-t')\dot{v}(t')dt' + \zeta(t)$ ,<sup>20</sup> where  $q$  and  $v$  are the coordinates and velocity of a Brownian particle. Model A displays only one minimum (Fig. 5, solid curve). Since the frequency factor of the barrier crossing rate very much depends on the characteristic of damping, the interplay of



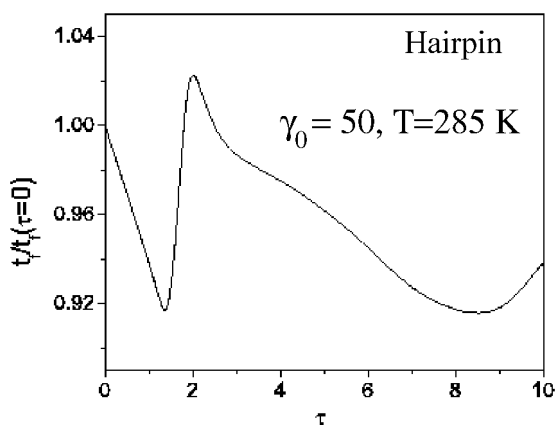


**Fig. 4** Plot of the renormalized folding time  $t_f/t_f(0)$  vs. the noise correlation times for the hairpin, where  $t_f(0)$  is the folding time in the Markovian limit,  $\tau = 0$ . We choose  $\gamma_0 = 50$  and  $T = 285$  K.  $t_f(0)$  for  $\gamma = 50$  is 37.6 ns.

frequency corresponding to the curvature of the potential well and the noise correlation time explains the minimum of the solid curve of Fig. 5.<sup>20,21</sup> It generally appears at low noise correlation time (Fig. 5). Then we may expect the first minimum in the protein folding kinetics due to the above reason. In other words, the first minimum occurs due to the interplay between the damping and the noise correlation time. In order to make this point more convincing, let us consider an ODF system where, in contrast to model A, the damping and colored noise are not related through FDR (eqn (4)) or the FDR is violated. We refer to this system as model B. For this model, we know that the mean lifetime increases as the noise correlation time grows for fixed noise strength when damping and colored noise have different origin.<sup>48,49</sup> This is because the frequency factor decreases and the effective barrier height increases.<sup>50,51</sup>

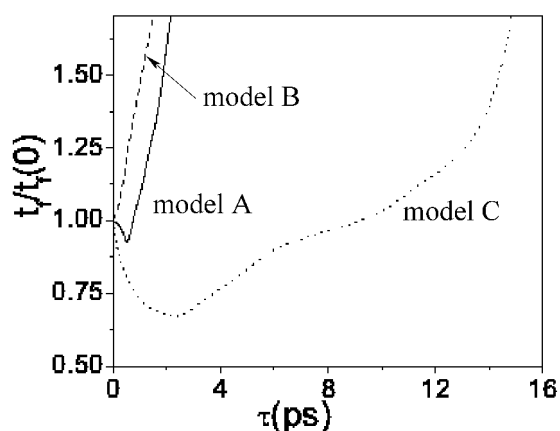


**Fig. 5** Plot of the re-normalized folding time  $t_f/t_f(0)$  vs. the noise correlation times for the ODF system both in the presence (model A) and the absence (model B) of FDR, and for  $\beta$ -hairpin in the absence of FDR (model C). Here  $t_f(0)$  is the folding time in the Markovian limit,  $\tau = 0$ .  $t_f(0) = 0.13$  ps, 0.19 ps and 2.56 ps for model A, B, and C, respectively. Results for the ODF systems at large values of  $\tau$  are not shown as  $t_f$  increases monotonically in that region. We choose  $\gamma_0 = 3.0$  and  $D = 2.0$ .

To demonstrate the variation of mean folding time with  $\tau$  for model B,  $t_f$  was calculated by solving the Langevin equation,<sup>48,49,51</sup>

$$m\dot{v} = q - q^3 - \gamma_0 v + \eta \quad (13)$$

and

$$\dot{\eta} = -\frac{\eta}{\tau} + \frac{\sqrt{D}}{\tau} \xi(t). \quad (14)$$

Here  $\eta(t)$  is colored Gaussian noise,  $\langle \eta(t)\eta(t') \rangle = D \exp(-|t - t'|/\tau)/\tau$ , where  $D$  is the noise strength which is independent of  $\gamma_0$ . The result is plotted in Fig. 5 (dashed curve). It shows that mean folding time increases monotonically with the noise correlation time. Here it is to be noted that the typical noise  $\eta(t)$  had been considered for activated barrier crossing problem and other aspects.<sup>52–60</sup> Thus, the results shown in Fig. 5 for models A and B support our conjecture that the first minimum at low  $\tau$  occurs as a result of interplay between the damping and colored noise.

Now we come to the second minimum. The distinct feature of the protein folding kinetics and the barrier crossing dynamics in the ODF system is that in the former case the barrier crossing dynamics is associated with the entropy of activation. Since the variance of the noise decreases with increase of noise correlation time (see the FDR, eqn (4)), the fluctuations in configurational entropy during the barrier crossing may decrease as  $\tau$  grows. It leads to a search for the native state with short folding time. Thus one would expect an additional minimum in protein folding kinetics to connect of damping, entropy and frequencies of multi-dimensional potential energy well. If it is really true then one may expect a single minimum in the protein folding kinetics in the presence of damping and colored noise such that they are not related through FDR. To check this expectation we consider protein folding kinetics in the presence of the same kind of environment as in model B (eqn (13) and (14)). Then the equation of motion becomes

$$m\ddot{r} = \bar{F}_c - \gamma_0 \dot{r} + \eta(t), \quad (15)$$

where  $\eta(t)$  obeys eqn (14). This is a Go model for proteins,<sup>32</sup> but we assume that the FDR given by eqn (4) does not hold. We refer to this model as model C. One of possibilities for violation of FDR is that the random and dissipative forces become independent having different origins. To convince it let us take a simple example. There is an electrical instrument which is associated with obvious mechanical damping and it can be driven by an electrical current. The current may be noisy in both direction and magnitude. The auto correlation time of electrical force or noise intensity may be varied by an experimentalist keeping fixed mechanical friction since the noise and damping have different origin. This kind of environment (absence of FDR relation) was considered in ref. 48, 49, 52–60. It may be found in biological system if an additional fluctuating force appears other than from a thermal origin. Effective dynamical contribution of biomolecules in the surroundings to the biosystem may be considered as the additional fluctuating force. Then total fluctuating force and damping should not follow the FDR relation. Furthermore, if

the temperature is very low then it should exactly correspond to the above example. However, we invoke the model C as the hypothetical one for the present context. It does not mean that in the original system the breakdown of FDR is possible. Therefore we have considered it just to demonstrate whether the interplay of damping, noise correlation time and configurational entropy can set up a minimum in the absence of FDR. Solving eqn (15) for model C, we observed a single minimum (dotted curve in Fig. 5) for the plot of  $t_f$  vs.  $\tau$ . It is really a surprising result with respect to the observation in model B where entropy of activation is absent. This observation can only be explained if we consider the configurational diffusion which may reduce the mean folding time as mentioned above. It implies that depending upon the difference between  $\gamma_0$  and  $\tau$  the interplay of damping, noise correlation time and configurational entropy can set up a minimum for a given noise strength. This kind of interplay one would expect in the present study also and the extent of the deviation (of the mean folding time from Kramers' theory) may depend on that. Thus the appearance of one more additional minimum in the variation of mean folding time with noise correlation time in the presence of a non-Markovian thermal bath is due to the interplay between damping, colored noise and entropy of activation. The dynamics of a multi-dimensional protein chain may experience the non-Markovian thermal bath in the following way. Progress toward the folded state relies on a large number of independent dihedral angle isomerization, each of which can be thought of as a single, elemental barrier-crossing event. Simulation showed<sup>10</sup> that the dynamics of these individual events are quite complex. Dihedral isomerization in longer peptides remains diffusional but the isomerization rate did not vary inversely with solvent damping strength,  $\gamma_0$ . This occurs because dihedral angle transition in neighboring residues are interdependent processes that occurs roughly on similar time scales which are of the order of picosecond (solvent relaxation time). This leads to complex (non-Markovian) diffusional dynamics,<sup>31</sup> which may not obey Kramers' theory. Thus an experimentalist would observe a mean folding time corresponding to collective non-Markovian dynamics around both minima for a given protein and make an explanation based on Fig. 2 and 3 to rationalize any deviation in mean folding time from Kramers' theory.

#### Departure from Kramers' behavior: evidence from folding simulations

Having used several viscogens, including glucose and glycerol to monitor the viscosity, Cellmer *et al.*<sup>15</sup> have shown that the thermal folding rate of the ultrafast-folding protein villin obeys eqn (1) but with parameter  $\xi > 0$ . The increase of the effective viscosity was attributed to the internal friction which reduces the diffusion coefficient due to increased free energy landscape roughness.

Here we want to examine how the colored noise modifies the effective solvent viscosity. In order to get unbiased results we have performed simulations not only for villin, but also for barstar and the hairpin. Fig. 6 shows the viscosity dependence of the folding rate,  $\kappa_f = 1/t_f$ , obtained for the protein barstar using the Markovian and NMD. One can show that the best fit

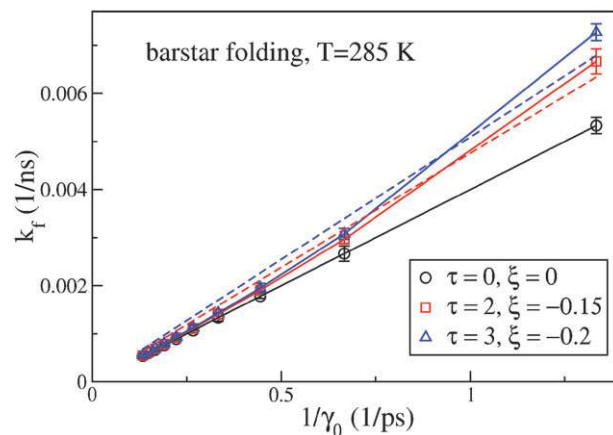


**Fig. 6** The dependence of the folding rate  $\kappa_f = 1/t_f$  on  $\gamma_0$  for barstar in the relatively low friction regime,  $0.75 \leq \gamma_0 \leq 7.5$ . The circles refer to the Markovian dynamics ( $\tau = 0$ ). Other legends correspond to non-Markovian dynamics ( $\tau \neq 0$ ). The solid lines refer to the fit given by eqn (1), where  $C = 0.004$ . The departure from Markovian dynamics is characterized by nonzero values of the parameter  $\xi$ , as shown by squares.  $\tau$  and  $\xi$  are measured in ps. The dashed lines correspond to the fit by eqn (12). For  $\tau = 2$  ps, we have fitting parameter  $\tilde{k}_0 = 0.0047$  and  $\lambda_r = 1.5 \times 10^{-9} \text{ ps}^{-1}$ . For  $\tau = 3$  ps, we have  $\tilde{k}_0 = 0.005$  and  $\lambda_r = 5 \times 10^{-7} \text{ ps}^{-1}$ . The results are averaged over 100 trajectories.

is given by eqn (1), where the constant  $C = 0.004$ , and  $\xi = 0, -0.15$  and  $-0.2$  ps for  $\tau = 0, 2$  and  $3$  ps, respectively. The dashed lines in Fig. 6 show the fit by eqn (12) with two free parameters  $\lambda_r$  and  $\tilde{k}_0$  the values of which are given in the figure caption. It shows that the approximate rate theory accounts for the deviation from Kramers' result relatively well.

Fig. 7a shows the viscosity dependence of the folding rate of  $\beta$ -hairpin for various values of  $\tau$  and  $1 \leq \gamma_0 \leq 30 \text{ ps}^{-1}$ . Again, as in the barstar case, the empirical formula (1) provides a better fit compared Grote-Hynes theory. The fitting parameters are  $C = 0.7$  and  $\xi = 0, -0.17, -0.25$  and  $-0.3$  ps for  $\tau = 0, 0.3, 2$  and  $3$  ps, respectively.

Since the departure from Kramers' behavior shown in Fig. 6 and 7a was obtained in the low enough friction regime, it is not clear if this remains valid in the overdamped limit, where the experiments<sup>14</sup> were performed. To check this, we calculated folding rates for the  $\beta$ -hairpin using viscosity values which are close to the experimental ones (Fig. 7b). For  $\tau = 0, 5, 10$  ps, we obtained  $\xi = 0, -2.02$  and  $-3.31$  ps, respectively. Therefore, non-Kramers' behavior also occurs in the high viscosity regime for this short protein. Since the departure from Kramers' behavior in the overdamped limit is notably weaker than in the low-viscosity regime, our data, obtained from the Go model, do not rule out a possibility that the non-Kramers' behavior in this limit may be not related to the colored noise. It would be interesting to verify whether a more realistic model with non-native interactions could lead to the stronger effect.

Fig. 8 shows the viscosity dependence of the folding rate for villin, where  $1 \leq \gamma_0 \leq 100 \text{ ps}^{-1}$ . For this interval of friction, the white noise results obey Kramers' theory (black solid line). The fit by eqn (1) (solid red line) works pretty well for  $\tau = 5$  ps with  $\xi = -0.34$  ps. Similar to the barstar and hairpin case, the Grote-Hynes gives a nearly linear dependence (dashed line).

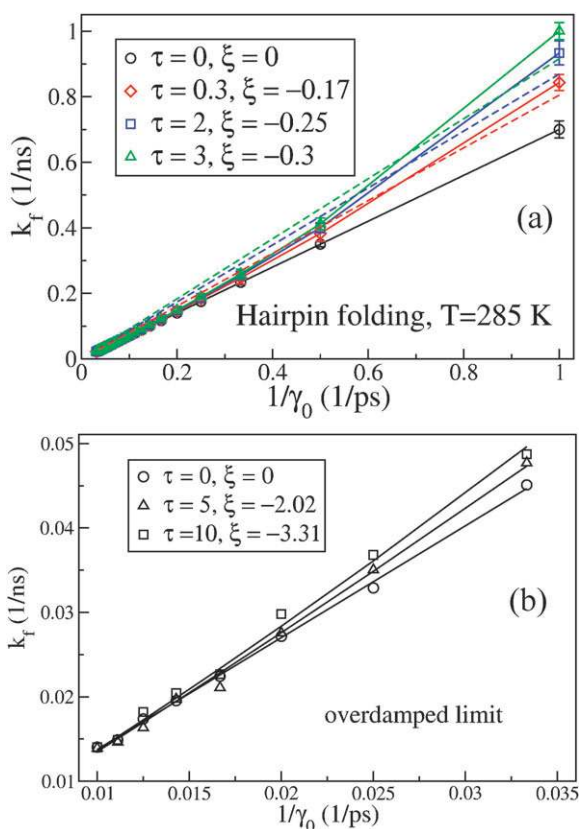


**Fig. 7** (a) The same as in Fig. 6, but for  $\beta$ -hairpin in the low friction regime,  $1 \leq \gamma_0 \leq 30 \text{ ps}^{-1}$ . The solid lines refer to the fit given by eqn (1), where  $C = 0.7$ . The departure from the Markovian dynamics is characterized by nonzero values of parameter  $\xi$ , as shown in boxes. The dashed lines are fits to eqn (12). The fitting parameter  $\tilde{k}_0 = 0.8, 0.87$  and  $0.92$  for  $\tau = 0.3, 2,$  and  $3 \text{ ps}$ , respectively.  $\lambda_r = 7.8 \times 10^{-6}, 5 \times 10^{-7},$  and  $5 \times 10^{-7} \text{ ps}^{-1}$  for  $\tau = 0.3, 2,$  and  $3 \text{ ps}$ , respectively. (b) The same as in (a) but for the high viscosity interval  $30 \leq \gamma_0 \leq 100 \text{ ps}^{-1}$ . The results are averaged over 1000 trajectories, and the error bars are smaller than the data symbols.

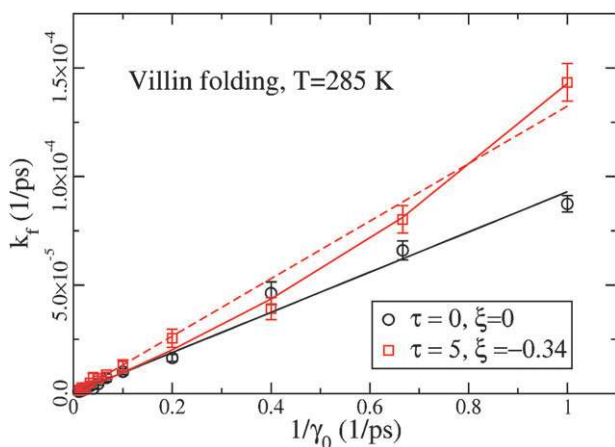


**Fig. 8** The dependence of the folding rate  $\kappa_f$  on  $\gamma_0$  for villin and  $1 \leq \gamma_0 \leq 100$ . Circles and squares refer to  $\tau = 0$  (Markovian dynamics) and  $5 \text{ ps}$  (NMD), respectively. The solid lines refer to the fit given by eqn (1), where  $C = 0.7$  and  $\xi = 0$  and  $-0.34 \text{ ps}$ . The dashed line is a fit to eqn (11) for  $\tau = 5 \text{ ps}$ , where  $\lambda = 1.1 \times 10^{-6} \text{ ps}^{-1}$  and  $\tilde{k}_0 = 0.00013$ .

Our results shown in Fig. 6–8 were obtained at  $T = 285 \text{ K}$ , where the folding is fast. The question we now ask is if the departure from Kramers' behavior remains valid at conditions which do not favor folding. To verify this, we have performed simulations at high temperatures ( $T = 664 \text{ K}$ ) which are believed to mimic these folding conditions. It turns out that the non-Kramers behavior (eqn (1)) remains valid in this case (Fig. 9). Thus, the NMD in the Go model can capture the departure from Kramers' behavior for any folding conditions.

The results from our thermal folding simulations (Fig. 6–9) unambiguously show that the effect of colored noise on folding kinetics may be described by eqn (1) with the negative phenomenological parameter  $\xi$ . This result is not compatible with the experimental results of Cellmer *et al.*<sup>15</sup> However, our simulation result is in accord with Grote–Hynes theory<sup>21</sup> because, as is evident from eqn (11), the folding rate should grow as  $\tau$  increases at least for some interval of viscosity and this results in negative values of  $\xi$ . The disagreement between the theory and the experiments<sup>15</sup> probably implies that the nature of departure from Kramers' theory with  $\xi > 0$  is not related to the memory effect.

#### Departure from Kramers' behavior: evidence from unfolding simulations

Recently, using two viscogens, xylose and glycerol to vary the viscosity, Pradeep and Udgaonkar,<sup>14</sup> *e.g.*, have shown that even in the overdamped limit the unfolding rate of the small protein barstar does not show an inverse dependence on the viscosity,  $\gamma_0$ , as expected from Kramers' theory. Instead, it is found to follow eqn (1), where the adjustable parameter  $\xi = -0.7 \text{ cP}$  and  $\xi = -0.5 \text{ cP}$  for xylose and glycerol cases, respectively. The reduction of solvent viscosity was assumed to be related to an internal friction.<sup>13,14</sup>

It should be noted that computation of non-Markovian unfolding rates of the 89-residue protein barstar in the overdamped limit is beyond our facilities. Let us explain this in

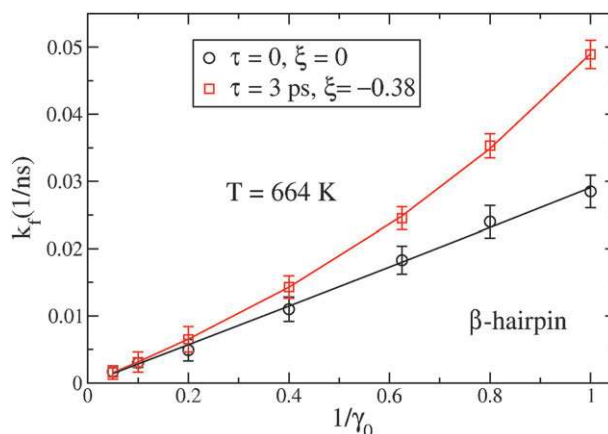


**Fig. 9** The viscosity dependence of the folding rate for  $\beta$ -hairpin at  $T = 664 \text{ K}$  (disfavored folding conditions). Fitting the simulation data to eqn (1) we obtain  $C \approx 0.03$ , and  $\xi = 0$  and  $-0.38$  for  $\tau = 0$  and  $3 \text{ ps}$ , respectively.

more detail. To study protein Markovian kinetics we have to solve the Langevin equation,

$$m \frac{d^2 r}{dt^2} = F_c - \gamma_0 \frac{dr}{dt} + \zeta(t),$$

where  $\zeta(t)$  is white noise. In the underdamped limit ( $\gamma_0 < 30 \text{ ps}^{-1}$ ) we can use, say, the Verlet algorithm with the time step  $\Delta t = 0.005\tau_L$  (see Models and Methods section). In the overdamped limit ( $\gamma_0 > 30 \text{ ps}^{-1}$ ), one can neglect the inertial term and the Langevin equation becomes  $\frac{dr}{dt} = \frac{1}{\gamma_0}(F_c + \zeta)$ . This equation may be solved using the simple Euler method which gives the position of a biomolecule at the time  $t + \Delta t$  as

$$x(\Delta t + t) = x(t) + \frac{\Delta t}{\gamma_0}(F_c + \zeta). \quad (16)$$

Due to the large value of  $\gamma_0$  we can choose the time step  $\Delta t = 0.1\tau_L$  which is 20-fold larger than the low viscosity case. Unfolding times in the overdamped limit are about two orders of magnitude larger than those in the low friction limit. However, the computation of  $t_{uf}$  in the former case is not much more CPU time demanding compared to the second one due to the use of the Euler method with the bigger time step  $\Delta t$ . The situation becomes very different if the dynamics are not Markovian. Because of the time dependence of the friction kernel (eqn (5)), in the overdamped limit, only for the corresponding Langevin equation cannot be rewritten in the form similar to eqn (16). As a result, we must also use the time step as small as in the low viscosity limit,  $\Delta t = 0.005\tau_L$ , and the computation of  $t_{uf}$  slows down by about two orders of magnitude compared to the Markovian case. Having relatively modest computational facilities, we are not able to obtain reliable results for barstar for many values of  $\gamma_0$  and  $\tau$  within reasonable amount of time. Therefore, we leave this problem for future studies.

Instead, we have studied the thermal unfolding of the shorter polypeptide chain  $\beta$ -hairpin at  $T = 450 \text{ K}$ . The

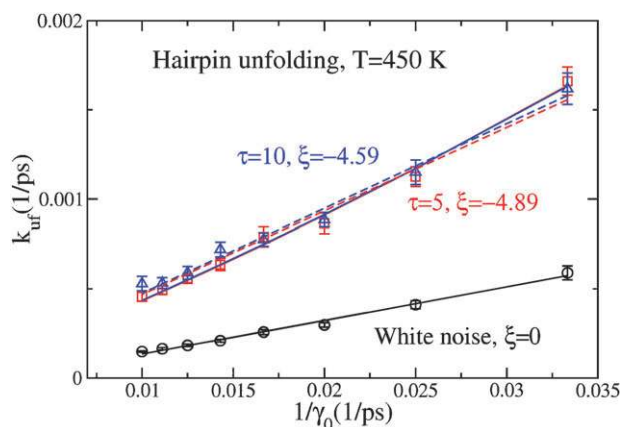


**Fig. 10** The viscosity dependence of the unfolding rate for  $\beta$ -hairpin at  $T = 450 \text{ K}$ . The Kramers' theory holds for the white noise case (circles). Fitting the simulation data to eqn (1) (solid lines) we obtain  $C \approx 0.04$ , and  $\xi = -4.89$  and  $-4.59$  for  $\tau = 5$  and  $10 \text{ ps}$ , respectively. The fit by eqn (12) (dashed lines) gives  $\tilde{k}_0 = 0.047$  and  $\lambda_r = 1.1 \times 10^{-5} \text{ ps}^{-1}$  for  $\tau = 5 \text{ ps}$ , and  $\tilde{k}_0 = 0.047$  and  $\lambda_r = 1 \times 10^{-5} \text{ ps}^{-1}$  for  $\tau = 10 \text{ ps}$ .

unfolding rates, obtained for different values of  $\tau$ , are presented in Fig. 10. As in the folding case, perfect Kramers' behavior is observed for the white noise case (solid black line). Fitting to the eqn (1), gives  $\xi = -4.89$  and  $-4.59$  for  $\tau = 5$  and  $10 \text{ ps}$ , respectively. This result agrees well not only with Grote-Hynes theory but also with the experimental data.<sup>14</sup> Eqn (12) gives almost the linear fit (Fig. 10), which is a little bit worse compared to the empiric formula (1).

Although computation of non-Markovian unfolding rates of barstar in the overdamped limit were not carried out yet, the non-Kramers behavior is also expected to hold for this protein as it should not depend on the number of amino acids. Therefore, our theoretical results support the scenario that the non-trivial behavior comes from the memory effect which speeds up the folding/unfolding process.

The folding experiments of Cellmer *et al.*<sup>15</sup> suggested that the internal friction enhances the free energy landscape roughness leading to  $\xi > 0$ . This result contradicts the picture proposed in ref. 14, where the effective viscosity is reduced. It is not entirely clear what scenario is superior as results probably depend on experimental conditions used by different groups. In our Go model, the relative thermodynamic stability of a protein does not depend on the viscosity, but the colored noise changes the folding kinetics in such a way that it can mimic the negative internal viscosity, if any. Fitting simulation results, obtained by Zagrovic and Pande<sup>9</sup> and Best and Hummer<sup>10</sup> to eqn (1) for the white noise, yields a negligible internal friction.<sup>15</sup> This also points to the important role of colored noise in non-Kramers folding/unfolding kinetics.

Before leaving this aspect we would like to note that in Fig. 6–10 we assume the same noise correlation for a range of viscosities for a particular curve. Practically, for each  $\gamma_0$  we should consider two different noise correlation times corresponding to two minima (Fig. 2 and 3). The smaller of them is independent of viscosity, since it is solely governed by the dynamics around the barrier top. But the bigger one may vary with the viscosity as discussed in the context of Fig. 2 and 3. However, it is difficult to include the effect of both the noise correlation times simultaneously in a theoretical model. Therefore, to check whether the breakdown of Kramers' theory is due to NMD or not, we have studied mean folding times considering a noise correlation time for a wide range. However, our calculation implies that the breakdown of Kramers' theory may be due to NMD and it may qualitatively account the experimental results obtained for different viscosity of the solvent. Another point to be mention here is that by fitting our result with eqn (1) for  $\xi < 0$  we mean that the effective frictional force may be reduced due to NMD. In other words the NMD is the origin of negative damping  $\xi$ . Now we come to the point how this is possible? Kramers' theory is based on the ordinary Langevin equation which neglects the correlation time of the solvent forces acting on the reactive motion. But when the motion takes place on a picosecond or subpicosecond time scale, the solvent forces at two different times can become correlated, *i.e.*, memory effects become important and Kramers' theory can break down. Under these circumstances, bath modes of high frequency have an important role and there should be a cut-off in the frequency distribution. This corresponds to the NMD. Then



dynamics does not experience damping from bath modes of low frequency region and effective friction is less (which may be one of the reasons for the breakdown of Kramers' theory) compared to Markovian dynamics. Thus NMD bears a signature of negative damping with respect to Markovian one. Our calculation also supports that. But it does not mean that NMD may be frictionless. Therefore, to avoid any confusion regarding divergence of eqn (1) one may comment that this equation is not valid for small damping, because in this case the barrier crossing rate is proportional to damping.<sup>27</sup>

## Conclusions

Using a generalized Langevin equation of motion for protein chains, we have investigated the role of NMD on their folding kinetics for both short and long proteins. Our observations imply the following points:

(a) The correlated noise may lead to the departure from the prediction of Kramers' theory for the viscosity dependence of folding and unfolding rates. Our results do not only explain experimental findings,<sup>13,14</sup> but also open a new way to solve this non-trivial problem.

(b) Surprisingly, the plot of  $t_f$  vs.  $\tau$  shows a double minima for proteins at any viscosity range. This implies that the protein folding dynamics experiences two different kind of frequency distribution of bath modes—one of them corresponding to fast dynamics around the barrier top and another one corresponding to the time scale which accounts how fast structural correlation varies with time. These observations have been obtained with the help of simple Go modeling. Inclusion of non-native contacts and other factors like side chains and water may lead to quantitative changes, but we believe that they will qualitatively remain valid for all biomolecules.

To our best knowledge, in this paper, we have made a first theoretical attempt to explain the violation of Kramers' theory for the dependence of protein folding rates on viscosity, using the colored noise theory. Our study has led to qualitatively novel results which are potentially interesting for experts from various fields of research.

## Acknowledgements

We thank M. Kouza for many useful discussions. This work was supported by the Ministry of Science and Informatics (grant No 202-204-234), National Science Council in Taiwan under grant numbers NSC 93-2112-M-001-027 and 95-2119-M-002-001, and Academia Sinica in Taiwan under grant numbers AS-92-TP-A09 and AS-95-TP-A07.

## References

- J. N. Onuchic and P. G. Wolynes, *Curr. Opin. Struct. Biol.*, 2004, **14**, 70–75.
- E. I. Shakhnovich, *Chem. Rev.*, 2006, **106**, 1559–1588.
- J. D. Bryngelson, J. N. Onuchic, N. D. Socci and P. G. Wolynes, *Proteins: Struct., Funct., Genet.*, 1995, **21**, 167.
- D. Thirumalai and S. A. Woodson, *Acc. Chem. Res.*, 1996, **29**, 433–439.
- M. S. Li and M. Cieplak, *Phys. Rev. E: Stat. Phys., Plasmas, Fluids, Relat. Interdiscip. Top.*, 1999, **59**, 970–976.
- M. Cieplak, T. X. Hoang and M. S. Li, *Phys. Rev. Lett.*, 1999, **83**, 1684–1687.
- M. S. Li, D. K. Klimov, J. E. Straub and D. Thirumalai, *J. Chem. Phys.*, 2008, **129**, 175101.
- D. K. Klimov and D. Thirumalai, *Phys. Rev. Lett.*, 1997, **79**, 317–320.
- B. Zagrovic and V. S. Pande, *J. Comput. Chem.*, 2003, **24**, 1432–1436.
- R. B. Best and G. Hummer, *Phys. Rev. Lett.*, 2006, **96**, 228104–228107.
- D. K. Klimov, D. Newfield and D. Thirumalai, *Proc. Natl. Acad. Sci. U. S. A.*, 2002, **99**, 8019–8024.
- R. van den Berg, R. Wain, C. M. Dobson and R. J. Ellis, *EMBO J.*, 2000, **19**, 3870–3879.
- K. W. Plaxco and D. Baker, *Proc. Natl. Acad. Sci. U. S. A.*, 1998, **95**, 13591–13596.
- L. Pradeep and J. B. Udgaonkar, *J. Mol. Biol.*, 2007, **366**, 1016–1028.
- T. Cellmer, E. R. Henry, J. Hofrichter and W. A. Eaton, *Proc. Natl. Acad. Sci. U. S. A.*, 2008, **105**, 18320–18325.
- L. Qui and S. J. Hagen, *Chem. Phys.*, 2004, **307**, 243–249.
- A. Ansari, C. M. Jones, E. R. Henry, J. Hofrichter and W. A. Eaton, *Science*, 1992, **256**, 1796–1798.
- J. Kubelka, T. K. Chiu, D. R. Davies, W. A. Eaton and J. Hofrichter, *J. Mol. Biol.*, 2006, **359**, 546–553.
- D. L. Hasha, T. Eguchi and J. Jonas, *J. Chem. Phys.*, 1981, **75**, 1571–1573.
- P. Hanggi, H. Talkner and M. Borkovec, *Rev. Mod. Phys.*, 1990, **62**, 251–341.
- R. F. Gorte and J. T. Hynes, *J. Chem. Phys.*, 1980, **73**, 2715–2732.
- P. Hanggi and F. Mojtabai, *Phys. Rev. A: At., Mol., Opt. Phys.*, 1982, **26**, 1168–1170.
- B. Bagchi and D. W. Oxtoby, *J. Chem. Phys.*, 1983, **78**, 2735–2741.
- S. P. Velsko and G. R. Fleming, *J. Chem. Phys.*, 1982, **76**, 3553–3562.
- S. P. Velsko, D. H. Waldeck and G. R. Fleming, *J. Chem. Phys.*, 1983, **78**, 249–258.
- K. M. Kerry and G. R. Fleming, *Chem. Phys. Lett.*, 1983, **93**, 322.
- H. A. Kramers, *Physica*, 1940, **7**, 284–298.
- M. R. Hurle, G. A. Michelotti, M. M. Crisanti and C. R. Matthews, *Proteins: Struct., Funct., Genet.*, 1987, **2**, 54–63.
- W. Teschner, R. Rudolph and J. R. Garel, *Biochemistry*, 1987, **26**, 2791–2796.
- T. Kleinert, W. Doster, H. Leyser, W. Petry, V. Schwarz and M. Settles, *Biochemistry*, 1998, **37**, 717–733.
- S. S. Plotkin and P. G. Wolynes, *Phys. Rev. Lett.*, 1998, **80**, 5015–5018.
- C. Clementi, H. Nymeyer and J. N. Onuchic, *J. Mol. Biol.*, 2000, **298**, 937–953.
- M. S. Li, M. Kouza and C. K. Hu, *Biophys. J.*, 2007, **92**, 547–551.
- S. T. Thomas, V. V. Loladze and G. I. Makhatazde, *Proc. Natl. Acad. Sci. U. S. A.*, 2001, **98**, 10670–10675.
- J. P. Hansen and I. R. McDonald, *Theory of Simple Liquids*, Academic, London, London, 1976.
- S. Okuyama and D. W. Oxtoby, *J. Chem. Phys.*, 1986, **84**, 5830–5835.
- T. Veitshans, D. K. Klimov and D. Thirumalai, *Folding Des.*, 1997, **2**, 1–22.
- M. P. Allen and D. Tildesley, *Computer Simulations of Liquids*, Clarendon, Oxford, 1987.
- M. Kouza, C. F. Chang, S. Hayryan, T. H. Yu, M. S. Li, T. H. Huang and C. K. Hu, *Biophys. J.*, 2005, **89**, 3353–3361.
- M. S. Li, C. K. Hu, D. K. Klimov and D. Thirumalai, *Proc. Natl. Acad. Sci. U. S. A.*, 2006, **103**, 93–98.
- M. Kouza, M. S. Li, C. K. Hu, E. P. O. Jr. and D. Thirumalai, *J. Phys. Chem. A*, 2006, **110**, 671–676.
- M. S. Li, *Biophys. J.*, 2007, **93**, 2644–2654.
- H. J. Fang, Y. Z. Chen, M. S. Li, C. L. Chang, Y. L. Hsu, T. H. Huang, H. M. Chen, T. Y. Tsong and C. K. Hu, *Biophys. J.*, 2009, **96**, 1892.
- M. Kouza, M. S. Li and C. K. Hu, *J. Chem. Phys.*, 2008, **128**, 045103.
- J. C. Smith, *Q. Rev. Biophys.*, 1991, **24**, 227–291.
- J. B. Asbury, T. Steinel, K. Kwak, S. A. Corselli, C. P. Lawrence, J. L. Skinner and M. D. Fayer, *J. Chem. Phys.*, 2004, **121**, 12431–12446.

- 47 M. S. Li, D. K. Klimov and D. Thirumalai, *Polymer*, 2004, **45**, 573–579.
- 48 C. Mahanta and T. G. Venkatesh, *Phys. Rev. E: Stat. Phys., Plasmas, Fluids, Relat. Interdiscip. Top.*, 1998, **58**, 4141–4146.
- 49 B. C. Bag, *Eur. Phys. J. B*, 2003, **34**, 115–118.
- 50 P. Hanggi, F. Marchesoni and P. Grigolini, *Z. Phys. B: Condens. Matter*, 1984, **56**, 333–339.
- 51 M. K. Sen and B. C. Bag, *Eur. Phys. J. B*, 2009, **68**, 253.
- 52 K. M. Rattray and A. J. McKane, *J. Phys. A: Math. Gen.*, 1991, **24**, 4375–4395.
- 53 F. Moss and P. V. E. McClintock, *Noise in Nonlinear Dynamical System*, Cambridge University Press, England, 1989.
- 54 J. Masoliver and J. M. Porra, *Phys. Rev. E: Stat. Phys., Plasmas, Fluids, Relat. Interdiscip. Top.*, 1993, **48**, 4309–4319.
- 55 S. J. B. Einchcomb and A. J. McKane, *Phys. Rev. E: Stat. Phys., Plasmas, Fluids, Relat. Interdiscip. Top.*, 1994, **49**, 259–266.
- 56 W. Horsthemke, C. R. Doering, T. S. Ray and M. A. Burschka, *Phys. Rev. A: At., Mol., Opt. Phys.*, 1992, **45**, 5492–5503.
- 57 C. R. Doering and J. C. Gadoua, *Phys. Rev. Lett.*, 1992, **69**, 2318–2221.
- 58 M. Bier and R. D. Astumian, *Phys. Rev. Lett.*, 1993, **71**, 1649–1652.
- 59 P. Hanggi, *Chem. Phys.*, 1994, **180**, 157–166.
- 60 P. Reiman and P. H. Roland Bartussekxi, *Chem. Phys.*, 1998, **235**, 11–26.